

# Pressure-induced structural transition of double-walled carbon nanotubes

X. Ye

*Surface Physics Laboratory and Department of Physics, Fudan University, Shanghai 200433, China*

D. Y. Sun

*Department of Physics, East China Normal University, Shanghai 200062, China*

X. G. Gong

*Surface Physics Laboratory and Department of Physics, Fudan University, Shanghai-200433, China*

(Received 18 January 2005; published 21 July 2005)

We demonstrate a hydrostatic pressure-induced structure transition of an isolated double-walled carbon nanotube using constant pressure molecular dynamics simulations. We find that, during the transition, the tube cross section is changed from circular to elliptical shape, associated with large reduction of radial bulk modulus. The transition pressure is essentially determined by the inner tube. The van der Waals interaction makes the inner tube and outer tube behave differently.

DOI: [10.1103/PhysRevB.72.035454](https://doi.org/10.1103/PhysRevB.72.035454)

PACS number(s): 61.46.+w, 61.48.+c, 62.50.+p, 78.30.Na

## I. INTRODUCTION

Since the discovery by Iijima,<sup>1</sup> carbon nanotube has been one of the most studied subjects in physics, chemistry, and materials science. Many interesting physical and chemical properties have been reported in the past years. Among them, the mechanical properties of the carbon nanotubes are very promising. Due to many potential applications as ultra-strong materials,<sup>2,3</sup> studies on the mechanical properties of carbon nanotube are still in progress.

It was found that along the axial direction, carbon nanotubes can be as hard as diamond.<sup>4</sup> Recently much attention has been paid to the elastic properties in the radial direction. By applying an external pressure,<sup>5–14</sup> the experiments showed that the carbon nanotubes can be very flexible and are much softer in the radial direction than in the axial direction. In the high-pressure Raman experiments,<sup>5–8</sup> it was found that the Raman intensity decreases dramatically beyond a few GPa, which was attributed to the pressure-induced structure transformation. In a similar experiment, Peters *et al.* found the radial breathing mode of carbon nanotubes disappeared at approximate 1.7 GPa.<sup>5</sup> The changes of the Raman intensity are reversible upon unloading the pressure. An x-ray diffraction study on single-walled carbon nanotube bundles under the pressure<sup>9</sup> showed a reversible disappearance of the triangular lattice at about 1.5 GPa. The neutron diffraction<sup>10</sup> also suggested that nanotube bundles undergo a cross-section deformation under the pressure.

On the theoretical side, constant pressure molecular dynamics (MD) simulations<sup>15–18</sup> were carried out on either isolated single-walled carbon nanotubes (SWCNTs) or SWCNT bundles. We have studied both isolated SWCNTs and SWCNT bundles under external pressure<sup>17,18</sup> and found that hydrostatic pressure can induce a hard-to-soft transition in SWCNTs associated with a circular to elliptical shape change of the cross section. For the isolated SWCNTs, the phase transition pressure is determined by the radius of the tube ( $\sim 1/R^3$ ), while for SWCNT bundles, the transition pressure depends on its radius as well as the symmetry.

Multi-walled carbon nanotubes (MWCNTs) are dominant products in the synthesizing process of carbon nanotube and they have broad ranges of potential applications.<sup>21–23</sup> Although SWCNTs under pressure have been widely studied by both experiments and simulations, to our best knowledge, the experimental and theoretical studies on the mechanical properties of MWCNTs under the external pressure are very scarce. After extensive studies on the SWCNTs, the natural question is how the MWCNTs behave under the external pressure, is it similar to or much different from SWCNTs? Among the MWCNTs, the double-walled carbon nanotube (DWCNT) is the simplest. Recently, it has shown that DWCNTs can also be easily synthesized by breaking the C<sub>60</sub> molecules encapsulated in SWCNTs.<sup>19</sup> The invention of new synthesis method will stimulate extensively experimental and theoretical investigation on DWCNTs. Very recently, DWCNTs under hydrostatic pressure have been studied by Puech *et al.*, their experimental results showed that the pressure coefficient from the inner tube is 45% smaller than from the outer tube.<sup>20</sup> So, the interaction between the inner and the outer tube would probably complicate the response of DWCNTs to the external pressure. In the present paper, using the constant-pressure molecular dynamics method for finite system,<sup>24</sup> we have studied the structures of DWCNTs with hydrostatic pressure and found a similar structural transition as observed in SWCNTs and SWCNT bundles.

This paper is organized as follows. The computational details are described in Sec. II. The calculated results are presented in Sec. III. Summary remarks are given in Sec. IV.

## II. COMPUTATIONAL DETAILS

Our simulations are performed on five DWCNTs, (10,10)@(15,15), (9,9)@(14,14), (8,8)@(13,13), (7,7)@(12,12) and (6,6)@(11,11), in which the distance between outer and inner tube is 3.3–3.4 Å, very close to the ideal layer spacing of graphite. The periodic boundary condition is employed in the axial direction to mimic infinitely

TABLE I. Calculated properties of double-walled carbon nanotubes (DWCNTs),  $\bar{d}_{in}$  and  $\bar{d}_{out}$ , the average bond length of the inner and the outer tube, respectively,  $R_{in}$  and  $R_{out}$ , the radius of the inner and outer tube, respectively, and  $t$ , the spacing distance between the two tubes. The values in brackets are for the isolated single-walled carbon nanotubes. The critical transition pressure ( $P_c$ ) and bulk moduli ( $B$ ) of DWCNTs are also shown.

DWCNTs	$\bar{d}_{in}$ (Å)	$\bar{d}_{out}$ (Å)	$R_{in}$ (Å)	$R_{out}$ (Å)	$t$ (Å)	$P_c$ (GPa)	$B$ (GPa)
(6,6)@(11,11)	1.4222 (1.4214)	1.4175 (1.4202)	4.0961 (4.0914)	7.4404 (7.4683)	3.3443	5.80	139
(7,7)@(12,12)	1.4219 (1.4209)	1.4173 (1.4201)	4.7722 (4.7655)	8.1129 (8.1448)	3.3407	3.56	129
(8,8)@(13,13)	1.4218 (1.4206)	1.4172 (1.4200)	5.4492 (5.4404)	8.7857 (8.8215)	3.3365	2.45	124
(9,9)@(14,14)	1.4217 (1.4204)	1.4171 (1.4200)	6.1267 (6.1160)	9.4590 (9.4984)	3.3323	1.80	121
(10,10)@(15,15)	1.4216 (1.4203)	1.4170 (1.4199)	6.8045 (6.7920)	10.1326 (10.1753)	3.3281	1.35	118

long tubes without any caps. The supercell contains 13 unit cells along the axial direction, which is about 32 Å. Since the tube is much harder in the axial direction than in the radial direction, in all the studies, the lengths in the axial direction are fixed. The constant pressure molecular dynamics method developed for finite systems<sup>24</sup> was used to simulate the structural changes for isolated DWCNTs under external pressure. Pressure is applied on the outer tube directly; it is transferred to the inner tube through the van der Waals forces between the two tubes. The equilibrium structure at zero temperature was obtained by the simulated annealing method. Most simulations are carried out at 300 K, where the system temperature is kept by using a Nosé-Hoover thermostat.<sup>25</sup>

The equations of motion are solved by using the standard velocity Verlet algorithm. In all the dynamics simulations, the time step is set as 1.0 fs. At each pressure, the system is allowed to run 100 ps for equilibrium, then the trajectories are collected for the analysis.

The Tersoff-type many-body potential<sup>26</sup> with the parameters given by Brenner<sup>27</sup> is used for the covalent interactions between carbon atoms. This potential has been widely used to simulate diamond, graphite, carbon nanotubes, and many hydrocarbon complexes.<sup>28–32,35</sup> The intertube and intratube van der Waals interactions are modelled by the Lennard-Jones (LJ) potential,  $V_{vdW} = C_{12}/r^{12} - C_6/r^6$ , where  $C_6 = 20 \text{ eV Å}^{-6}$  and  $C_{12} = 2.48 \times 10^4 \text{ eV Å}^{-12}$ .<sup>33,34</sup> This approach has been successfully used to describe the mechanical properties and the phase transition of SWCNT bundles.<sup>17</sup> The cutoff of LJ potential is set as 15 Å in present work.

### III. RESULTS AND DISCUSSIONS

The stable structures of DWCNTs at zero temperature and zero pressure are obtained by the simulated annealing method. In this process, the DWCNTs are first equilibrated at 300 K using the molecular dynamics simulation, then the temperature is slowly cooled down to zero. Consequently, both inner tube and outer tube rotate relatively to each other

to reduce the potential energy. After the full relaxation, we have found that the cross sections of the two tubes remain an almost perfect circle, but the radius of the tubes is slightly changed. The structural properties are shown in Table I. Due to a different potential model, generally we obtain a small bulk modulus, comparing with that obtained by Lu.<sup>36</sup> Our calculation shows that the bulk modulus is sensitive to the radius of the tube. Because of the attractive effect of the van der Waals potential, the outer tube shrinks and the inner tube expands compared with the radius of the isolated SWCNT, thus the distance between the two tubes is slightly decreased.

The simulations at different pressure show that all DWCNTs undergo a pressure-induced structure transition, in which the cross sections of inner and outer tubes are changed from circular-like to elliptic-like. Figure 1 shows the evolution of the tube cross section with increasing the external pressure for the (9,9)@(14,14) tube. It can be seen that, as the pressure is lower than 1.8 GPa, the cross section stays circular-like, while the cross section is changed to elliptical-like when the pressure is higher than 1.8 GPa. At the pressure of  $\sim 1.8$  GPa, the structure transition can be clearly observed. Similar transition has been found in other studied DWCNTs. This kind of transition is similar to that obtained for SWCNTs under the external pressure in previous studies.<sup>18</sup> To further confirm the structure change, we have also calculated the length of the long axis and short axis of the cross section for both inner and outer tubes at different pressure, which are also plotted in Fig. 1. At small pressure, the long and short axes of tubes have almost the same length, while after the transition, the long axis increases and the short axis decreases as a result of shape transformation. If increasing pressure further, the elliptical shape changes to a dumbbell shape.

Figure 2 presents the reduced volume of the DWCNTs as a function of the external pressure. The obvious discontinuity of the slopes in the pressure-volume plot indicates that the bulk moduli has a jump between the circular-like and elliptical-like structure. The phase with circular shape at low pressure is much harder than the phase with elliptic shape at

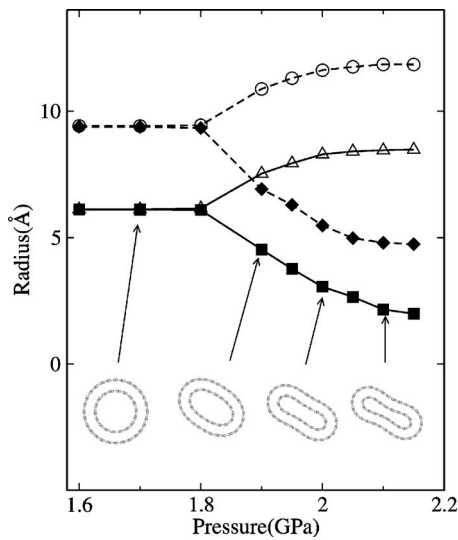


FIG. 1. The radius of the tube as a function of pressure for the (9,9)@(14,14) nanotube. The dashed line is for outer tube, the solid line for inner tube. The open legend is for long radius, the solid legend for short radius. The shape of cross section at pressure = 1.7, 1.9, 2.0, 2.1 GPa is shown. At the same pressure, the outer tube and inner tube simultaneously collapse from circle-like to elliptical-like.

high pressure. Thus one can consider it as a pressure-induced hard-soft transition, similar to that found in isolated SWCNT. By calculating the slope of the volume-pressure curve in Fig. 2, we find that the bulk moduli for the *hard* phase (circle shape) is almost two orders in magnitude larger than that for the *soft* phase (elliptic shape).

We show the transition pressure as a function of the tube radius in Fig. 3; for comparison the results for the isolated

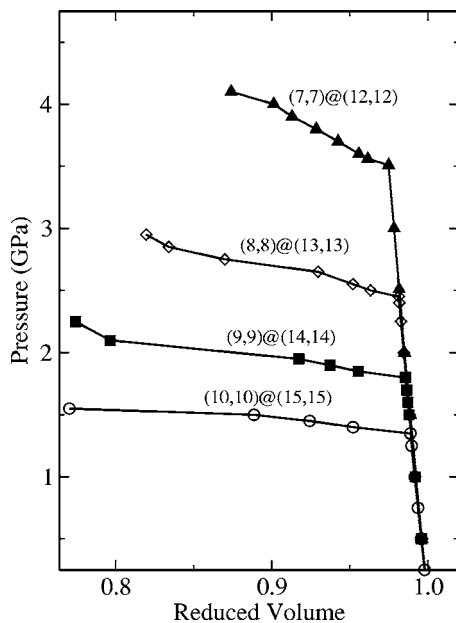


FIG. 2. Pressure as a function of the reduced volume for DWCNTs at 300 K. The volume is renormalized by the volume at zero pressure. The discontinuity of the slopes indicates hard-soft transition under hydrostatic pressure.

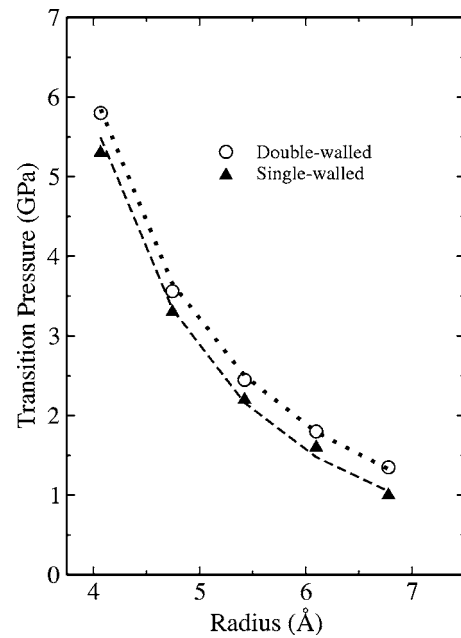


FIG. 3. Transition pressure as a function of radius of nanotubes at 300 K. The radius of the inner tube is used as the radius of the DWCNT. The transition pressure of both SWCNTs and DWCNTs is proportional to  $\sim 1/R^3$  (indicated by the dashed line and dotted line, respectively).

SWCNTs are also shown. It can be seen that the transition pressures are strongly dependent on the radius of tubes. The smaller the radius, the higher the transition pressure. The transition pressure of DWCNTs is only slightly higher than that of the SWCNTs with the same radius of the inner tube, which suggests that the transition pressure of the DWCNTs is essentially determined by the inner tube. In fact, this can be easily understood by noticing that the inner tube with smaller radius is much *harder* than the outer tube. If we consider the DWCNT as a pseudo-single-walled nanotube with effective thickness, the elastic behavior of the DWCNT can be discussed in terms of the continuum elastic theory. Similar to what has been done in the previous work for SWCNTs,<sup>18</sup> the transition pressure of DWCNTs decreases with increasing tube radius in a third power law. If the radius of the inner tube is used, the fitting to the third power law gives the effect thickness of  $\sim 1.0$  Å, compared with 0.66 Å in SWCNTs.<sup>35</sup>

The structure transition of DWCNTs is also reflected in the changes of bond lengths for both inner and outer tubes, as shown in Fig. 4. The obvious difference of bond lengths between inner tube and outer tube can be clearly observed even at the zero pressure. As the pressure increases, the bond lengths decrease linearly for both inner and outer tube. It is interesting to notice that the inner tube and outer tube show different behavior for the changes of the bond length near the transition. The structure transition accompanies a sudden increase of the bond length of the outer tube. After the transition, the bond length of the outer tube suddenly increases, while the bond length of the inner tube continues to decrease up to a slightly larger pressure, then increases slowly.

We first address why the changes of the bond length for the inner tube show different behavior from the outer tube.

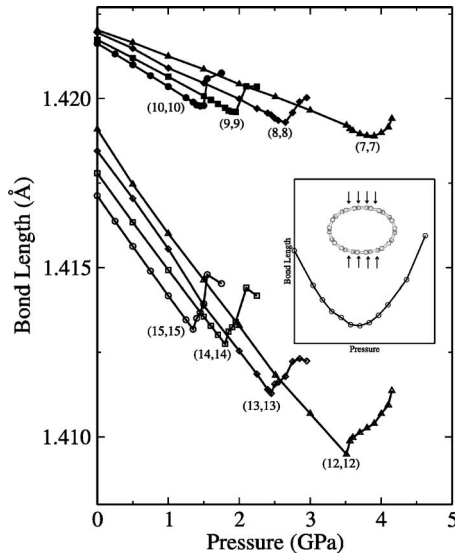


FIG. 4. The bond length as a function of the hydrostatic pressure. The open legend is for the outer tube, solid legend for the inner tube. The inset shows the behavior of the single-walled tube bond length under a uniaxial pressure. The similar behavior for the inner tube and the tube under the uniaxial pressure can clearly be observed.

Upon loading a hydrostatic pressure, the outer tube collapses first, after that a nonuniform van der Waals force acts on the inner tube, which makes the average bond length changes of the inner tube different from that of the outer tube. Thus the structure transition of the outer tube is driven by the hydrostatic pressure, while the transition of the inner tube is driven by an uniaxial pressure. To confirm that the hydrostatic pressure and uniaxial pressure will lead to different behavior of the bond length change, we have simulated a SWCNT under an uniaxial pressure. In this simulation, the uniaxial pressure also drives the circular tube to the elliptical-like; no sudden change of the bond length can be observed, as shown in the insert of Fig. 4, which is very similar to the behavior of the inner tube.

The increase of the bond length after the transition can be understood as following. The structure transition is the result of the competition between the internal energy of the carbon nanotube and the external pressure. The internal energy favors having a circle shape, while the external pressure intends to reduce the volume. The volume of the tube can be reduced in two ways, either decreasing the bond length or deforming the bond angle. At small pressure, the volume of the tube is reduced by decreasing the bond length while the bond angle is not changed in order to keep the circle shape due to the symmetry. After the phase transition, the volume can be reduced more efficiently by deforming the bond angle. So, after the transition, the increasing of the bond length can release significant elastic energy while the reduction of the volume can be achieved by changing the bonding angle. This is also why the structure becomes very soft after the transition.

To make this point more clear, we provide a simple elastic model to explain the phenomenon of the tube under the hydrostatic pressure. Considering an uniform tube, whose cross

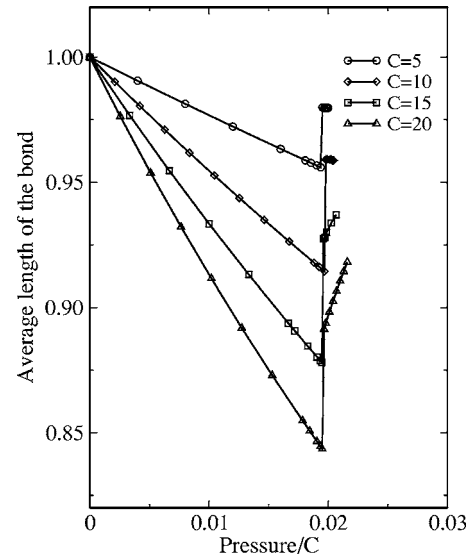


FIG. 5. The average bond length as a function of pressure scaled with elastic constant for bond angle ( $C$ ). After the polygon collapses, the average bond length increases.

section is a polygon with  $n$  atoms ( $N=30$ ), the free energy per length of the model system can be written as

$$F = PS + \frac{1}{2}C \sum_i \theta_i^2 + \frac{1}{2}D \sum_i (l_i - L)^2,$$

where  $P$ ,  $S$ , and  $C(D)$  are the pressure, the area of the polygon, and the elastic constants for the bond angle (length),  $\theta_i$  is the  $i$ th bond angle,  $l_i$  is the  $i$ th bond length, and  $L$  is the equilibrium bond length at zero pressure. We use the conjugate gradient method to minimize  $F$  to get the most energetically favorable bond length and bond angle under the pressure. We find the similar shape transition in such a simple model system. The average bond length decreases with the increasing pressure, as shown in Fig. 5, and suddenly increases soon after the polygon collapse. The larger the  $C$ , the larger the transition pressure. In fact, the transition pressure can be scaled with the elastic constant of the bond angle, as shown in Fig. 5. One can also see that the larger elastic constant  $C$  leads to a large change of the bond length, which is the result of the competition between the changes in the bond angle and the bond length.

#### IV. SUMMARY

By using the constant pressure molecular dynamics method specially developed for a finite system, we have studied the structure of isolated DWCNTs under external pressure. We find that pressure-induced structure transition takes place in all the studied DWCNTs. The critical transition pressure is strongly dependent on the radius of the inner tube. The different behavior for the outer tube and inner tube has been identified: the outer tube is very similar to the transition of SWCNTs under a hydrostatic pressure, while the inner tube is similar to transition under a uniaxial pressure.



## ACKNOWLEDGMENTS

X.Y. thanks D. Zhang and X.H. Zhang for the discussion. This work is partially supported by the National Science Foundation of China, the special funds for major state basic

research. D.Y.S. is also partially supported by Shanghai Municipal Education Commission and Shanghai Education Development Foundation. The computation was performed at the Shanghai Supercomputer Center and the Supercomputer at Fudan.

- <sup>1</sup>S. Iijima, *Nature (London)* **354**, 56 (1991).
- <sup>2</sup>M. S. Dresselhaus, G. Dresselhaus, and P. C. Eklund, *Science of Fullerenes and Carbon Nanotubes* (Academic, New York, 1996).
- <sup>3</sup>B. Vigolo, A. Penicaud, C. Coulon, C. Sauder, R. Pailler, C. Journet, P. Bernier, and P. Poulin, *Science* **290**, 1331 (2000); R. H. Baughman, *ibid.* **290**, 1310 (2000).
- <sup>4</sup>M. M. J. Treacy, T. W. Ebbesen, and J. M. Gibson, *Nature (London)* **381**, 678 (1996).
- <sup>5</sup>M. J. Peters, L. E. McNeil, J. P. Lu, and D. Kahn, *Phys. Rev. B* **61**, 5939 (2000).
- <sup>6</sup>U. D. Venkateswaran, A. M. Rao, E. Richter, M. Menon, A. Rinzler, R. E. Smalley, and P. C. Eklund, *Phys. Rev. B* **59**, 10928 (1999).
- <sup>7</sup>A. K. Sood, Pallavi V. Teredesai, D. V. S. Muthu, Rahul. Sen, A. Govindaraj, and C. N. R. Rao, *Phys. Status Solidi B* **215**, 393 (1999).
- <sup>8</sup>P. V. Teredesai, A. K. Sood, D. V. S. Muthu, Rahul. Sen, A. Govindaraj, and C. N. R. Rao, *Chem. Phys. Lett.* **319**, 296 (2000).
- <sup>9</sup>J. Tang, L. C. Qin, T. Sasaki, M. Yudasaka, A. Matsushita, and S. Iijima, *Phys. Rev. Lett.* **85**, 1887 (2000).
- <sup>10</sup>S. Rols, I. N. Gontcharenko, R. Almairac, J. L. Sauvajol, and I. Mirebeau, *Phys. Rev. B* **64**, 153401 (2001).
- <sup>11</sup>R. Gaál, J. P. Salvetat, and L. Forró, *Phys. Rev. B* **61**, 7320 (2000).
- <sup>12</sup>J. Tang, L. C. Qin, T. Sasaki, M. Yudasaka, A. Matsushita, and S. Iijima, *J. Phys.: Condens. Matter* **14**, 10575 (2002).
- <sup>13</sup>S. A. Chesnokov, V. A. Nalimova, A. G. Rinzler, R. E. Smalley, and J. E. Fischer, *Phys. Rev. Lett.* **82**, 343 (1999).
- <sup>14</sup>S. Kazaoui, N. Minami, H. Yamawaki, K. Aoki, H. Kataura, and Y. Achiba, *Phys. Rev. B* **62**, 1643 (2000).
- <sup>15</sup>S. P. Chan, W. L. Yim, X. G. Gong, and Z. F. Liu, *Phys. Rev. B* **68**, 075404 (2003).
- <sup>16</sup>J. A. Elliott, J. K. W. Sandler, A. H. Windle, R. J. Young, and M. S. P. Shaffer, *Phys. Rev. Lett.* **92**, 095501 (2004).
- <sup>17</sup>X. H. Zhang, D. Y. Sun, Z. F. Liu, and X. G. Gong, *Phys. Rev. B* **70**, 035422 (2004); X. H. Zhang, Z. F. Liu, and X. G. Gong, *Phys. Rev. Lett.* **93**, 149601 (2004).
- <sup>18</sup>D. Y. Sun, D. J. Shu, M. Ji, Feng Liu, M. Wang, and X. G. Gong, *Phys. Rev. B* **70**, 165417 (2004).
- <sup>19</sup>D. E. Luzzi and B. W. Smith, in *Science and Application of Nanotubes*, edited by D. Tomanek and R. J. Enbody (Kluwer, New York, 2000), p. 67.
- <sup>20</sup>P. Puech, H. Hubel, D. Dunstan, R. R. Bacsá, C. Laurent, and W. S. Bacsá, *Phys. Rev. Lett.* **93**, 095506 (2004).
- <sup>21</sup>Q. Zheng and Q. Jiang, *Phys. Rev. Lett.* **88**, 045503 (2002).
- <sup>22</sup>S. B. Legoas, V. R. Coluci, S. F. Braga, P. Z. Coura, S. O. Dantas, and D. S. Galvão, *Phys. Rev. Lett.* **90**, 055504 (2003).
- <sup>23</sup>G. Chen, S. Bandow, E. R. Margine, C. Nisoli, A. N. Kolmogorov, Vincent H. Crespi, R. Gupta, G. U. Sumanasekera, S. Iijima, and P. C. Eklund, *Phys. Rev. Lett.* **90**, 257403 (2003).
- <sup>24</sup>D. Y. Sun and X. G. Gong, *J. Phys.: Condens. Matter* **14**, L487 (2002).
- <sup>25</sup>S. Nosé, *Mol. Phys.* **52**, 255 (1984); W. G. Hoover, *Phys. Rev. A* **31**, 1695 (1985).
- <sup>26</sup>J. Tersoff, *Phys. Rev. Lett.* **61**, 2879 (1988).
- <sup>27</sup>D. W. Brenner, *Phys. Rev. B* **42**, 9458 (1990).
- <sup>28</sup>D. H. Robertson, D. W. Brenner, and J. W. Mintmire, *Phys. Rev. B* **45**, R12592 (1992).
- <sup>29</sup>M. B. Nardelli, B. I. Yakobson, and J. Bernholc, *Phys. Rev. Lett.* **81**, 4656 (1998).
- <sup>30</sup>Y. Xia, Y. Ma, Y. Xing, Y. Mu, C. Tan, and L. Mei, *Phys. Rev. B* **61**, 11088 (2000).
- <sup>31</sup>A. N. Kolmogorov and V. H. Crespi, *Phys. Rev. Lett.* **85**, 4727 (2000).
- <sup>32</sup>Y. Ma, Y. Xia, M. Zhao, R. Wang, and L. Mei, *Phys. Rev. B* **63**, 115422 (2001).
- <sup>33</sup>L. A. Girifalco and R. A. Lad, *J. Chem. Phys.* **25**, 693 (1956).
- <sup>34</sup>L. Henrard, E. Hernandez, P. Bernier, and A. Rubio, *Phys. Rev. B* **60**, R8521 (1999).
- <sup>35</sup>B. I. Yakobson, C. J. Brabec, and J. Bernholc, *Phys. Rev. Lett.* **76**, 2511 (1996).
- <sup>36</sup>J. P. Lu, *Phys. Rev. Lett.* **79**, 1297 (1997).